7th International Conference on Modelling and Simulation in Nuclear Science and Engineering (7ICMSNSE)
Ottawa Marriott Hotel, Ottawa, Ontario, Canada, October 18-21, 2015

7ICMSNSE-38

Development of Upgraded Full-Core 3D Diffusion Models for the Pickering Stations

B. Arsenault[1], Z. Ćatović[2], S. Shaula[1] and P.D. Buchan[3]
[1] AMEC Foster Wheeler, 4th Floor, 700 University Avenue, Toronto, Ontario, Canada M5G 1X6
[2] Ontario Power Generation, 889 Brock Road, 6th floor, Pickering, Ontario, Canada , L1W 3J2
[3] Ontario Power Generation, 1675 Montgomery Park Rd., Pickering, Ontario, Canada L1V 2R5
benoit.arsenault@amecfw.com, zlatko.catovic@opg.com, sergiy.shaula@amecfw.com, david.buchan@opg.com

Abstract

This paper describes a methodology used to model Pickering reactors with the Reactor Physics toolset currently in use at OPG stations, which includes the Reactor Physics Industry Standard Toolset (RFSP-IST/WIMS-IST/DRAGON-IST) and the fuel management code SORO.

Detailed geometries were modeled in DRAGON-IST with devices and structures that extended into the reflector region and incremental properties were calculated for reactivity devices, guide tubes and structural materials based on the engineering drawings.

Simulations and comparisons with measurements performed showed improved predictive capabilities of the new reactor physics models.

Keywords: Lattice-cell neutron transport model, Full-core diffusion model, Core-follow, Validation

1. Introduction

The Pickering Nuclear Generating Station A (PNGSA) from Ontario Power Generation (OPG) is comprised of 4 nominally identical reactors, of which Units 1 and 4 are currently operating. Each reactor consists of a core assembly and other systems designed to generate 1652 MW(th) power.

The current PNGSA full-core diffusion model for the Reactor Fuelling Simulation Program (RFSP-IST) [1], uses the incremental properties of in-core devices and structures derived by standard super-cell model from the 3D transport code DRAGON-IST [2], [3] and the MULTICELL computer code [4]. Burnup dependent, fuel and reflector lattice cell properties were derived with the 2D transport code WIMS-IST [5] and the ENDF/B-VI data library [6]. DRAGON-IST can solve the transport equations in 2D or 3D cylindrical geometries to calculate the 2-group properties of the lattice cells and the properties of the in-core devices. MULTICELL solves the diffusion equations using 3D rectangular geometries with current-to-flux ratios at the surface of strong absorbers to calculate the 1 ½-group properties of the in-core devices.

The incremental cross sections calculated with DRAGON-IST for the current PNGSA model are based on a two-lattice pitch model where absorbing devices are introduced between two mid-burnup

fuel bundles to calculate the incremental cross sections. It is obvious that such a model cannot be applied to materials passing through the reflector region. Recently an alternative approach which addresses the shortcoming mentioned above was assessed. In the alternative approach an extended configuration of lattice cells in DRAGON-IST was used to allow for separate homogenization of the incremental properties of the devices and materials in the core fuel lattice and in the reflector regions. The extended model includes the calandria wall, the reflector region and a few fuel channels.

The objective of this paper is to present the upgraded DRAGON-IST and the Reactor Fuelling Simulation Program (RFSP-IST) models for PNGSA and also, present some validation results. The exact same approach was also used for the Darlington Nuclear Generating Station (DNGS) from OPG which consists of four units each generating 2650 MW(th) of power. The new methodology showed the same benefits, however the paper focuses only on the PNGSA station.

2. General physical description of the PNGSA CANDU reactor

The core assembly consists of a horizontal notched cylinder oriented in the east-west direction. The cylinder consists of a larger diameter main shell, with two smaller sub-shells at either end. Attached to each of the sub-shells is an end-shield assembly. Closing the axial ends of the cylinder is the tube-sheet. The structure containing the main-shell, sub-shell, and the end-shield between the tube sheets is, generally considered to be the calandria.

At the inside surface of the main shell is a thermal shield consisting of steel plates 4 ½-inch thickness held approximately ½ inch from the inside surface of the main shell by support plates.

With the PNGSA calandria are 390 channels arranged in a rectangular lattice. These channels penetrate the tube sheet at both ends, and traverse the entire length of the calandria. The channels are comprised of an outer cylinder, the calandria tube, and an inner cylinder, the pressure tube. Within the annulus separating the pressure and calandria tubes is carbon dioxide, the annulus gas, and garter springs. Each PNGSA pressure tube contains 12 fuel bundles each comprised of 28 fuel elements.

Penetrating the calandria vertically are in-core flux detectors, adjuster and shutoff rods, and liquid-zone compartments. These devices are contained within guide tubes (for the detectors and rods) or liquid-zone assemblies. The intent of the guide tubes is to provide support and ensure the correct placement of the devices within the core. Each guide tube assembly is affixed to the thermal shield at the bottom of the core.

3. Upgraded full-core reactor model

The PNGSA core contains several reactivity devices and components which need to be modelled in RFSP-IST and SORO, the full-core diffusion codes. These devices and components include:

- Structural materials for the Adjuster Absorbers (AAs): locators, locator couplers, spring assemblies, un-perforated section of the in-core guide tubes,
- Adjusters and stainless steel cables and connectors,

- Structural materials for the Shut-Off Rods (SORs): locators, locator couplers, spring assemblies, un-perforated section of the in-core bottom guide tubes, perforated section of the in-core guide tubes,
- SORs, the stainless steel cables and connectors,
- Structural materials for the Liquid-Zone Controllers (LZCs); locators, locator couplers, un-perforated and perforated section of the in-core guide tubes,
- LZCs, drained and filled configurations,
- Structural materials for thee Neutron Flux Monitors (NFMs),
- Garter Springs, and
- Moderator inlet nozzles.

3.1 Methodology

A number of steps were followed to upgrade the DRAGON-IST and RFSP-IST models. The first step was to calculate the homogenized macroscopic cross sections of the materials in the extended super-cell model with DRAGON-IST. All the super-cell calculations in DRAGON-IST were based on the 89 energy-group ENDF/B-VI data library. The second step was to use the homogenized incremental properties correctly representing materials in the reflector regions and in the lattices in the upgraded RFSP-IST model of PNGSA. The third step was to extend the upgraded RFSP-IST model to the computer code Simulation Of Reactor Operation (SORO) **[7]**. Finally, validation exercises were performed to evaluate the new models.

3.1.1 2-dimensional configurations in DRAGON-IST

A 2-dimensional one-lattice pitch model enclosed in a square configuration with sides equal to 28.575 cm in length was used to calculate the lattice properties. The calculations were done with a critical buckling and Table 1 lists the dimensions that were used in the model. The WIMS-IST computer code was used to calculate the isotopic concentrations of the fuel at mid-burnup stage then further used by DRAGON-IST for 2-dimensional calculations. Isotopic concentrations of the fuel were representative of the whole core time-average burnup at a value of 4043.43 MWd/THe.

The 2-dimensional geometry was used to calculate the 33-energy-group macroscopic cross sections of the fuel, pre-homogenized in 3 cylindrical regions. 33 energy group cross sections of structural and absorber materials pre-homogenized into cylindrical regions were prepared as well, as required by the 3-dimensional DRAGON-IST model. A conversion of 3-dimensional lattice cells into 2-dimensional lattice cells was performed by conserving the material volumes and distances within the cell.

Table 1: Dimensions Used in the Lattice Model

Parameter	Value
Creep (%)	1.5
Pressure Tube Inner radius (cm)	5.26770
Pressure Tube Outer Radius (cm)	5.70489
Calandria Tube Inner Radius (cm)	6.55447
Calandria Tube Outer Radius (cm)	6.70941

3.1.2 3-dimensional configurations in DRAGON-IST

The PNGSA reactors consist of a cylindrical calandria made of stainless steel with a wall thickness of 1 inch (2.54 cm). Inside the calandria tank are stainless steel thermal slabs of a 4.5-inch (11.43 cm) that are welded to the wall. The radius of the reactor from its centre to the surface of the thermal slab is approximately 152.591 inches. A total of 11 rows of channels are centred in the core with a lattice pitch of 28.575 cm equivalent to a core radius of 314.325 cm, which leaves a reflector thickness of 73.256 cm.

Figure 1 shows a plane view of the model that was built in DRAGON-IST to represent the last two rows of fuel followed by the reflector, the stainless steel slab and the calandria wall. The extent of the model in the Z direction was equal to one-bundle length (49.53 cm).

The 3-dimensional geometry shown in Figure 1 was used to calculate the incremental properties of the structural materials located in the reflector region between the fuel channels and the stainless steel slabs. This model uses a more realistic flux profile in the reflector region to condense and homogenize the cross sections.

The extended super-cell calculations in 3-dimensions were all performed using a 33-energy-group structure and the final results were condensed into a two-energy-group structure with a cut-off at 0.625 eV. Two configurations were used to calculate each set of incremental cross sections:

1. The first configuration had four fuel channels, the reflector region, the slab and the calandria wall.
2. The second configuration consisted of the reference configuration to which the structural materials and absorbers were added.

Macroscopic incremental cross sections were calculated for each homogenisation region shown in Figure 1 by subtracting the reference set of macroscopic cross sections from the macroscopic cross sections calculated with the second configuration. Table 2 lists the incremental cross sections and homogenization volumes that were used to update the RFSP-IST and SORO models.

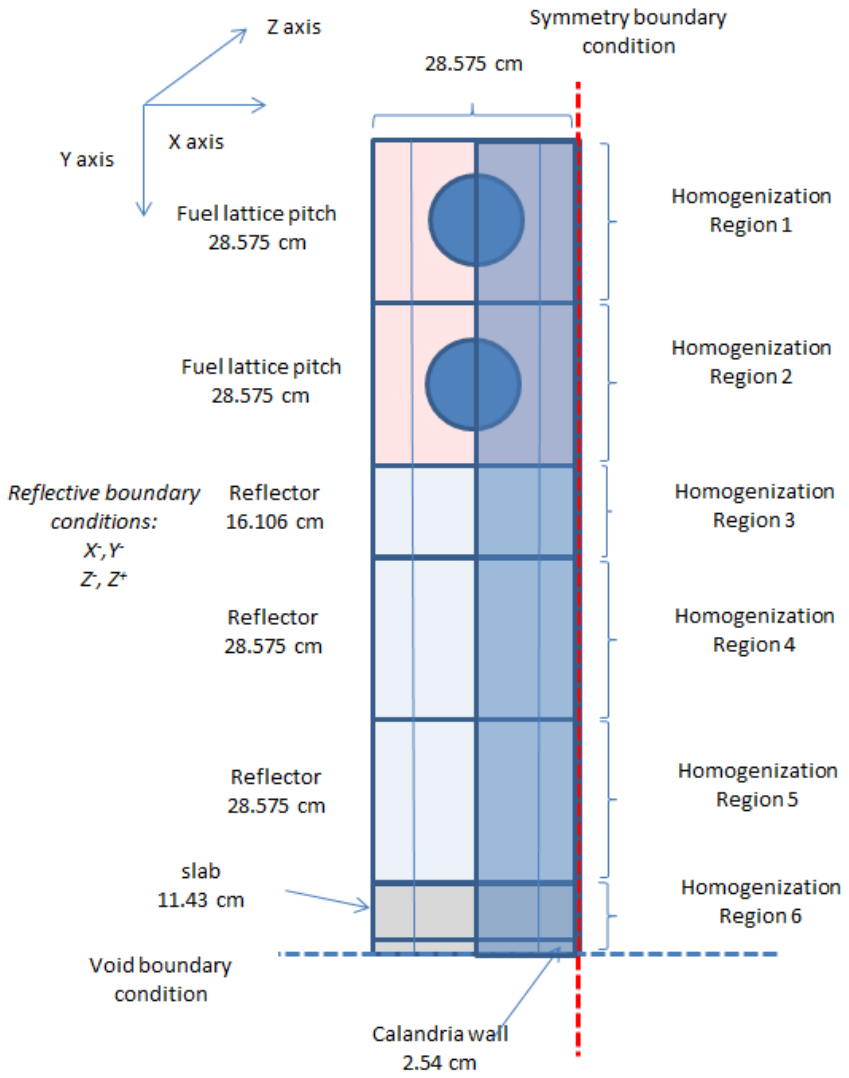

Figure 1: Plane View of the Reference Model Used in DRAGON-IST

Table 2: Incremental Cross Sections Calculated with DRAGON-IST with the Associated Homogenization Volumes

Incremental Set	Homogenization Volume*	Incremental Set	Homogenization Volume*
Perforated guide tubes	1	SORs 12-23 and cables	1,4
Adjusters and cables	1,4	Connectors for SORs	2
Structural materials	3,4,5	Structural materials SORs 1-11	3,4,5
Connectors for adjusters	2	Structural materials SORs 12-23	3,4,5
SORs 1-11	1	Inlet nozzles	5
Garter springs	1	NFMs structural materials	1,3,4,5
LZCs	1	Structural Materials	4,5

* See the homogenization volumes defined in Figure 1.

4. Benchmarking of the upgraded full-core model

The upgraded full-core reactor model does not rely on tuning of physical representation of reactivity devices and in-core materials. Instead, all the incremental cross sections were calculated with DRAGON-IST based on the specifications provided in the engineering drawings. The upgraded RFSP-IST and SORO models were benchmarked against reactivity perturbation test and FINCH power measurements and the results are documented in the next Sections.

4.1 Qualification based on reactivity perturbation test results

The objective was to calculate the Neutron Over-Power Protection (NOP) simulation errors associated with detector signals and the channel powers as predicted using the update PNGSA model. Since deficiencies in either the fundamental models, or the worth of devices, would lead to detector ratio or channel power errors, this exercise is used to quantify the accuracy of the current RFSP-IST model.

The analysis was carried out using data obtained from Pickering A Unit 1 and 4 and simulations performed using RFSP-IST. Station measurements of Flux Detector Responses (FDR) and FINCH powers, associated with 21 and 18 reactivity device perturbations respectively for Units 1 and 4 involving Liquid-Zone Controllers (LZCs), Shut-Off Rods (SORs) and Adjuster Absorbers (AAs) were taken during the commissioning of the Shut-Down System Enhancement (SDSE) system.

4.1.1 Background

The Pickering Shut-Down System Enhancement (SDSE) system employs 29 Neutron Over-Power Protection (NOP) detectors. These are arranged in three safety channels, G (10 detectors), H (9 detectors), and J (10 detectors). There are also 14 flux detectors associated with the Reactor Regulating System (RRS). These are associated spatially with the 14 liquid-zone controllers. The measurements used in the analysis to determine detector ratio error, take into account all 43 (29 NOP plus 14 RRS) flux detectors.

The Pickering A units each has 22 FINCHs capable of measuring the coolant flow, and the coolant inlet and outlet temperatures. From these measured quantities, channel power can be calculated using Equation 1. Figure 2 shows a face view of the reactor with the location of the FINCH channels.

$$CP_i = k \times F_{des} \times F_i \times \left[T_{out,i}^2 - T_{in,i}^2\right] \qquad (1)$$

Where,

k is an empirical constant of proportionality, units kW s / (kg $^oC^2$)

CP is the channel power, units kW

F_{des} is the mass flow for the channel as per design, units kg/s

F_i is i-th FINCH nominal flow, units dimensionless

$T_{out,i}$ is i-th FINCH measured channel outlet temperature, units ^oC

$T_{in,i}$ is i-th FINCH measured channel inlet temperature, units ^oC

As part of commissioning activities, reactivity perturbation tests were conducted for both Units 1 and 4. During these tests, reactivity devices of the LZCs were exercised in order to induce a change in the local flux/power. During these perturbations detector readings and FINCH data were recorded. The flux perturbations were produced by moving the following devices:

SORs Fully out to 50% inserted
AAs Fully inserted to fully withdrawn
LZCs 10% full to 90% full

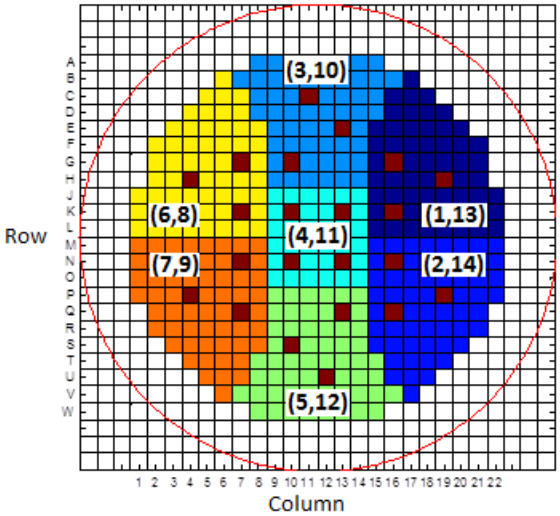

Figure 2: Color Coded map of Thermal Zones and FINCH Channel Locations Shown in Brown

4.1.2 Assumptions

The test were performed at 60% Full Power (FP) following a long shutdown. The assumed core conditions are given in Table 3 for both the Unit 1 and Unit 4 tests. Additional assumptions included:

- The incremental cross sections representing reactivity devices at reference core conditions are not significantly changed by the core conditions during the tests,
- Long shutdown corrected fuel burnup was used,
- ^{135}Xe was equilibrated at power prior to start of the tests. A major flux transient was not expected due to the short time (~10 min) for each flux perturbation.
- Static diffusion calculations were performed with the RFSP-IST code and therefore, the comparisons to the measured data were made at a time after the perturbations, at which time these transient responses are completed.

Table 3: Initial Core Conditions Used for the Post-Simulations of the SDSE Measurements

Parameter	Value	
	Unit 1	Unit 4
Coolant Density (g/cm^3)	0.854	0.854
Coolant Temperature (°C)	266.95	266.95
Moderator Temperature (°C)	67.8	68.0
Moderator Poison (ppm Boron)	0.18	0.68
Power (%FP)	60	58

The relative difference between the calculated and measured detector responses and channel powers were calculated using the RFSP-IST RDS for Pickering A Units 1 and 4. These calculations were used as a measure of the fitness for service of the new full-core model.

4.1.3 Methodology

For each test sequence, the analysis consisted of:

1. Establishment of the initial core conditions present at the start of the test sequence.
2. A sequence of static runs, with the device position, reactor power, and the time step being obtained from the available commissioning data.
3. At the beginning and end of each perturbation, the detector flux ratio and channel power ratio were obtained with the static calculations.
4. Steps 2 and 3 were repeated over the duration of each transient sequence.

Flux detector ratio error†, expressed in terms of flux, is defined as:

$$FDR_{error}(i,j) = \frac{\Phi_m(i,j,after)/\Phi_m(i,j,before) - \Phi_s(i,j,after)/\Phi_s(i,j,before)}{\Phi_m(i,j,after)/\Phi_m(i,j,before)} \quad (2)$$

Where,

i	index of flux detectors or FINCHs,
j	index of perturbation,
m	measured quantity,
s	simulated quantity,
after	quantities after a perturbation, and
before	quantities before a perturbation.

† Contribution from the detector cables was not included.

Channel power ratio error, expressed in terms of channel power, is defined as:

$$CPR_{error}(i,j) = \frac{CP_m(i,j,after)/CP_m(i,j,before) - CP_s(i,j,after)/CP_s(i,j,before)}{CP_m(i,j,after)/CP_m(i,j,before)} \quad (3)^{\ddagger}$$

FDR and CPR ratios were calculated with RFSP-IST for each perturbation case, at each detector location and for each FINCH channel. Final samples for the statistical analysis were formed of relative differences between measured and simulated flux ratios and power ratios ((measured-simulated)/measured).

4.2 Benchmarking of channel power distribution

The full-core model that was prepared in RFSP-IST was transferred into SORO, the computer code used for core-follow simulation purposes. The SORO model was used to perform simulations of reactor operations for Unit 1 and Unit 4 from 2008 to 2013 using the same channel fuelling sequences as production data. The results of the simulations were compared with the measurements from the 22 FINCH channels for the same period. The FINCH channels were grouped in thermal zone powers shown in Figure 2. Details of the simulations are provided in the sections below.

4.2.1 Methodology

Measurements were extracted from the data acquisition system at PNGSA for comparisons against the core-follow simulations of Unit 1 and Unit 4 from 2008 to 2013. The core-follow analysis was performed with the current SORO model used at the station for day-to-day operations and with the upgraded full-core model equivalent to the RFSP-IST model documented in Section 3. The primary parameter for the evaluation of the SORO models is the SORO FINCH Error (SFE) Spatial Standard Deviation (STD). The second Figure Of Merit (FOM) is the Average Standard FINCH Error (ASFE). The model with smaller SFE STD is generally considered a better model. Small ASFE is also desirable and ideally the nest model would have both, the SFE and the ASFE close to zero.

The data included in the acquisition system is listed below:

- Location of AAs,
- Level of each LZC,
- Time of the refuelling operations and number of bundles refuelled,
- Power level,
- Moderator boron and gadolinium concentrations,
- Moderator isotopic purity,
- Coolant isotopic purity,
- Average moderator temperature,

‡ See Equation 2 for a definition of the sub-indices.

- Average coolant temperature,
- Flows associated to each FINCH channel, and
- Inlet and outlet temperatures for each FINCH.

The parameters were used in SORO to calculate the power distribution as a function of time based on static calculations. The channel powers were compared with the measured values for the FINCH channels based on Equation 1.

5. Results

The sections below provide the code and model qualification results that were obtained with the improved full-core model for the commissioning test results and for the core-follow channel power benchmarking exercises, respectively.

5.1 Commissioning test results (RFSP-IST)

The flux detector ratios and the channel power ratios were evaluated for Pickering A Units 1 and 4, by comparison of the calculated values with RFSP-IST with the measured data. The errors were averaged over all devices[§] and the following results were obtained:

For Unit 1	Flux Detector Ratio Error	= -0.65 ± 1.23 %
	Channel Power Ratio Error	= -0.62 ± 2.07 %
For Unit 4	Flux Detector Ratio Error	= -0.54 ± 1.29 %
	Channel Power Ratio Error	= -0.54 ± 2.05 %

The first term represents the mean value of the percent difference in the measured minus the simulated results (systematic bias) while the second term is the standard deviation (random error). It is concluded that:

1. The calculated simulation errors have a negative systematic bias, and
2. The improved full-core model matches accurately the Pickering A core measurements.

5.2 Benchmarking of channel power distribution (SORO)

The ASFE and the standard deviations of the two models were assessed in this exercise. Unit 1 ASFE for the production and upgraded SORO models are 1.24% and 1.27%, respectively, while the standard deviations are 2.32% for the production SORO model and 2.19% for the upgraded SORO model. Unit 4 ASFE for the production and upgraded models are 0.24% and 0.19%, respectively, while the standard deviations are 2.16% for the production SORO model and 1.96% for the upgraded SORO model.

In terms of SFE standard deviations, it is apparent that the upgraded SORO model outperforms the production SORO model. These differences observed were consistent in time, as can be seen from Figure 3 below.

[§] A negative error means that the updated RDS overestimates the absorption of the reactivity devices.

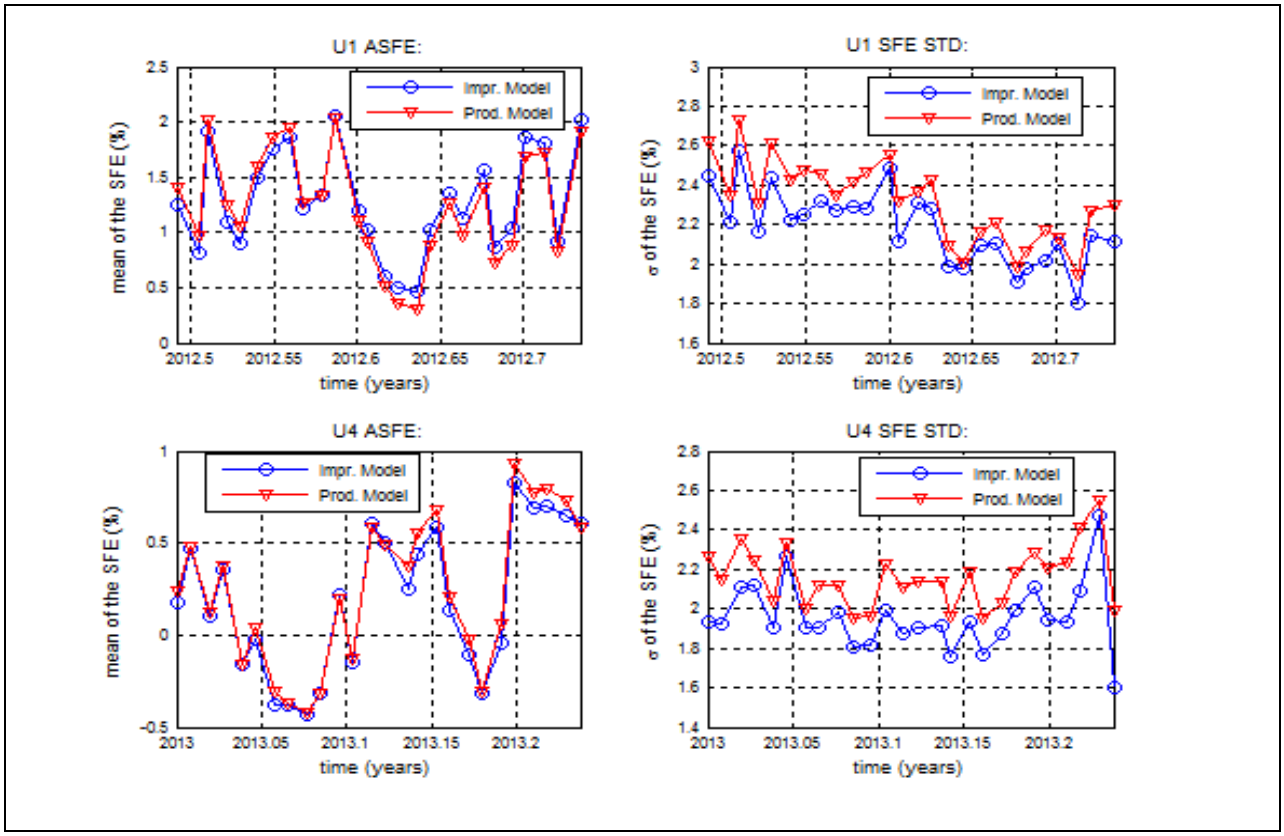

Figure 3: ASFE and SFE Standard Deviation for Units 1 and 4, with the Improved and the Production Models.

The comparison of individual SFE for FINCH's in zones 3/10, 4/11 and 5/12 are shown in Figure 4. Of particular importance are FINCH channels C11 in zone 3/10 and U12 in zone 5/12. For these channels SFE improvement is ~50%. For other channels SFE calculated with the improved and the production model are comparable.

SFE for Unit 1, Axial Zone Pair 3/10 FINCH's

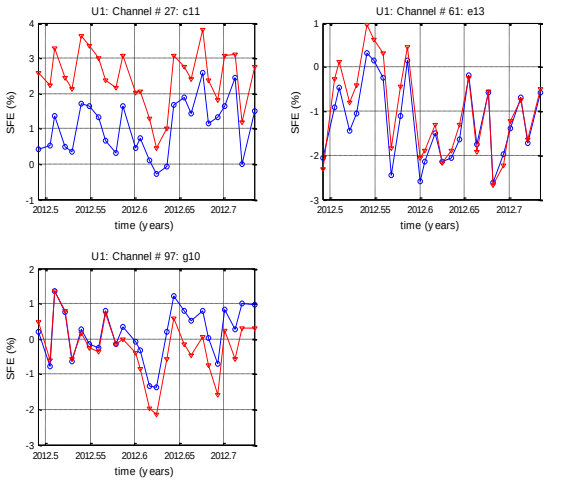

SFE** for Unit 4, Axial Zone Pair 3/10 FINCH's

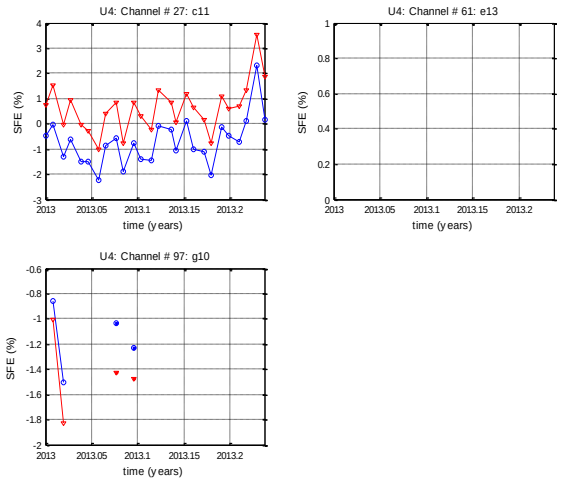

SFE for Unit 1, Axial Zone Pair 4/11 FINCH's

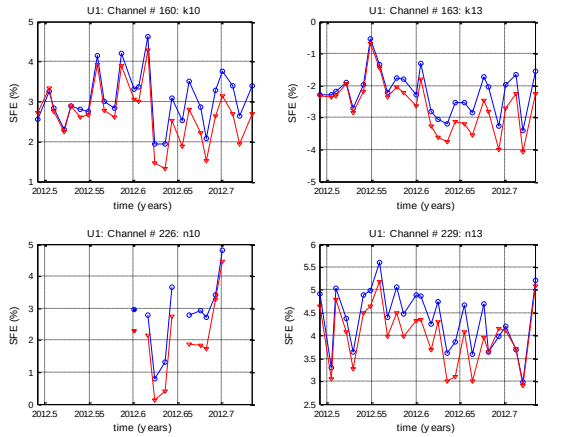

SFE for Unit 4, Axial Zone Pair 4/11 FINCH's

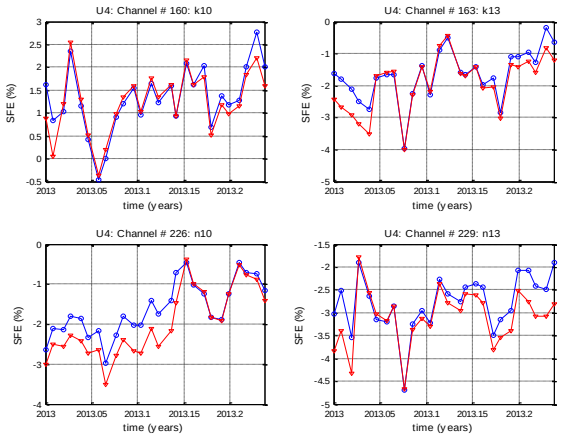

SFE for Unit 1, Axial Zone Pair 5/12 FINCH's

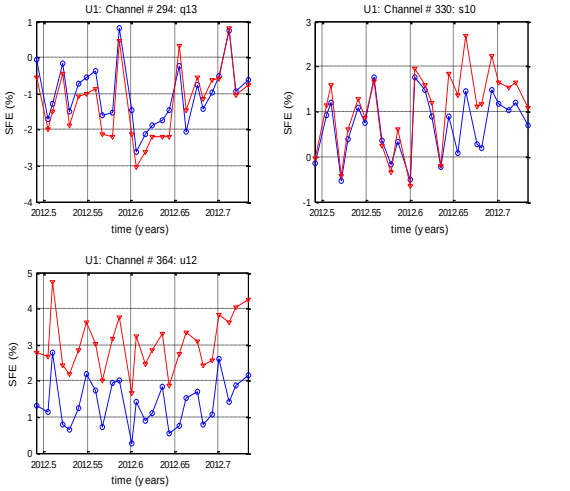

SFE for Unit 4, Axial Zone Pair 5/11 FINCH's

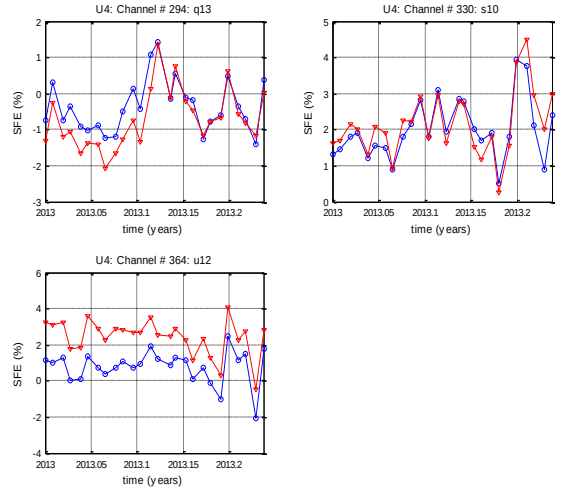

Figure 4††: SFE for Units 1 and 4, in Zones 3/10, 4/11 and 5/12.

** Standard deviation is not reported because measurements were irrational for that period.

†† The blue lines represent the upgraded model and the red lines represent the production model.

6. Conclusions

An upgraded full-core RFSP-IST model was built using on extended supercell configurations in DRAGON-IST to have a flux profile representative of the true location in the core and used to calculate the incremental cross sections of the devices. All the geometries that were built in DRAGON-IST were based on the engineering drawings.

The results of the analysis showed that the upgraded full-core RFSP-IST model matches accurately the PNGSA core measurements. The results of the analysis also showed that the improved model outperforms the existing model used in production.

Additional work has also been performed and showed that the new model improved the margins of operation compared to the existing model used in production. The work has not been presented due to the significant additional content that would be required in the paper.

7. References

[1] B. Rouben, "RFSP-IST, the Industry Standard Tool Computer Program for CANDU Reactor Core Design and Analysis", in Proceedings of the 13th Pacific Basin Nuclear Conference, Shenzhen, China, 2002 October 21-25.

[2] G. Marleau, A. Hébert and R. Roy, "A User Guide for DRAGON 3.04T", IGE-175, Rev. 5, August 2005.

[3] G. Marleau, "DRAGON Theory Manual, Part 1: Collision Probability Calculations", IGE-236, Rev. 1, October 2001.

[4] J.V. Donnelly et al., "Modeling CANDU Reactivity Devices with WIMS-AECL/MULTICELL and Super-homogenization", Proc. of 17th Annual Conference of Canadian Nuclear Society, Fredericton, New Brunswick, Canada, 1996 June 9-12.

[5] J.D. Irish and S.R. Douglas, "Validation of WIMS-IST", Proc. of 23rd Annual Conference of Canadian Nuclear Society, Toronto, Canada, 2002 June 2-5.

[6] P.J. Laughton and I.C. Gauld, "The Derivation of Burnup-Chain and Pseudo-Fission-Product Nuclear Data for a WIMS-AECL ENDF/B-VI-Based Cross-Section Library", Proc. of 18th Annual Conference of Canadian Nuclear Society, Pembroke, Ontario, Canada, 1994 October.

[7] C. Olive et al., "Upgrades to the Simulations of Reactor Operation (SORO) Code for Core-Follow Simulations of Ontario Power Generation and Bruce Power Reactors", IAEA Meeting, Korea, 2004.